

The irreproducibility of the measurements of the surface recombination velocity and the dark field effect is primarily due to a change in the center trap density. After repeated ambient cycles, the surface becomes more or less stabilized. However, the stability may be disturbed by long exposure to a wet atmosphere. The

effect of water vapor upon the germanium surface may involve some slow chemical processes. It would be of interest to see whether a thick oxide layer can provide a protection against water vapor.

The authors wish to thank Sumner Mayburg for helpful discussion and criticism of the manuscript.

Nuclear Magnetic Resonance in Semiconductors. II. Quadrupole Broadening of Nuclear Magnetic Resonance Lines by Elastic Axial Deformation

R. G. SHULMAN, B. J. WYLUDA, AND P. W. ANDERSON

Bell Telephone Laboratories, Murray Hill, New Jersey

(Received April 5, 1957)

Nuclear electric-quadrupole moments interact with electric-field gradients at the nucleus. In a perfect cubic crystal, the average gradients vanish and there are no quadrupolar interactions. Nuclear magnetic resonance studies of the semiconductors InSb and GaSb have revealed no quadrupolar interactions in our samples, indicating a high degree of crystalline perfection. By applying stresses to these crystals, we have been able to destroy the crystalline symmetry reversibly, thereby producing quadrupole broadening of the nuclear magnetic resonance lines. Strains of less than 10^{-4} have been detected and the resulting field gradients measured. The "gradient-elastic" proportionality constants connecting stress and field gradient are discussed in relation to crystal symmetry and have been deduced from the measurements.

INTRODUCTION

INTERACTIONS between nuclear electric-quadrupole moments and electric-field gradients at the nucleus have been shown to be responsible for many features of nuclear magnetic resonance lines in solids.¹ Line shapes, splittings, and relaxation times have been shown in certain cases to be determined by quadrupole interaction. Of course, there are many other kinds of nuclear interactions in solids and it is only under certain conditions that the quadrupole interactions will be dominant. One condition required for this interaction is that the electric-field gradient at the nucleus be nonvanishing. If the nuclear environment is cubic, there should not be any field gradients at the nucleus. Watkins and Pound,² however, have shown that quadrupole interactions were strong in their "good" alkali halide crystals. They attribute the presence of electric-field gradients to internal strains arising from crystal imperfections.

In previous investigations³ it had been indicated that samples of InSb, kindly supplied by Dr. H. J. Hrostowski, were perfect enough cubic crystals so that the effects of internal strain upon NMR (nuclear magnetic resonance) lines were negligible. Since the first-order quadrupole components of the In¹¹⁵ resonance had not been removed by internal strains, it was decided to deform the InSb crystal elastically in order to destroy the cubic symmetry and split the quadrupole compo-

nents. We were able to do this, and also to measure this splitting and relate it to the applied stress. Watkins and Pound attempted the same experiments in alkali halide crystals but were unsuccessful because, as mentioned above, they found that internal strains had already split the quadrupole components.

APPARATUS

A modified Pound-Knight-Watkins⁴ spectrometer was used in these experiments. The main modification was to replace the 6J6 oscillator tube by a General Electric GL-6072. Because of the lower gain of the GL-6072 it was necessary to use two tubes in parallel. The advantage of this circuit is that the GL-6072 generates less noise in the audio range than any other tube tested. Its disadvantage is the lower gain of the tube. The magnet is a Varian Associates six-inch electromagnet with a gap that was at various times $1\frac{1}{2}$ inches and $1\frac{3}{4}$ inches. In the smaller gap measurements were made with $H_0 \sim 8300$ oe while in the larger gap $H_0 \sim 6500$ oe. Since signal-to-noise was not very large all measurements were made at 77°K. Figure 1 represents the sample holder, coil, and pressure equipment. A single-crystal rod was placed in the inner phenolic fiber tube. Both ends of the sample rod were squared off with a diamond cutting wheel. No additional precautions were taken to insure purely axial forces. The bottom end of the sample rested on a fiber plug fastened in the fiber tube. A short piece of fiber rod was placed on

¹ R. V. Pound, Phys. Rev. **79**, 685 (1950).

² G. D. Watkins and R. V. Pound, Phys. Rev. **89**, 658 (1953).

³ Shulman, Mays, and McCall, Phys. Rev. **100**, 692 (1955).

⁴ G. D. Watkins, thesis, Harvard University, 1952 (unpublished).

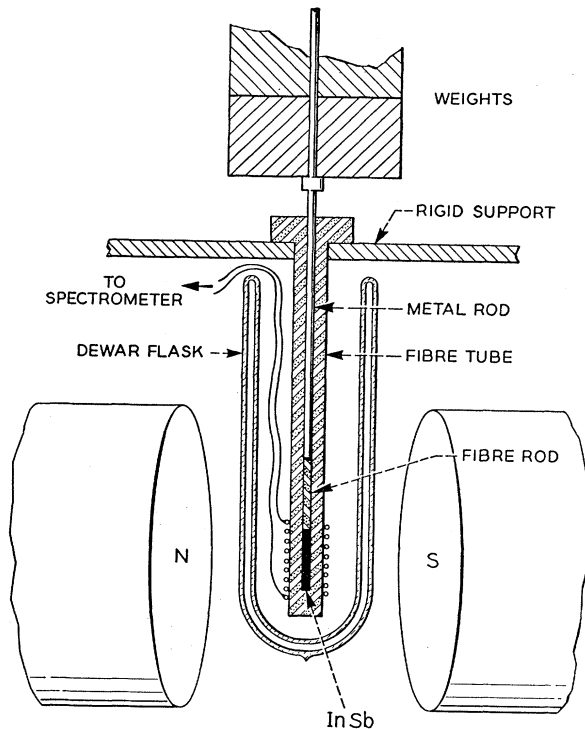


Fig. 1. Schematic diagram of sample holder and magnet showing method of applying stress.

top of the sample and on top of this a stainless steel rod transmitted the force from the weights.

EXPERIMENT

Measurements were made on two single crystals of InSb. In one the [110] axis was along the coil direction, and in the other the [010]. These samples were cut from crystals which were *n*-type extrinsic at 77°K with $(N_d - N_a) \sim 1 \times 10^{15}/\text{cm}^3$ and $(N_d + N_a)$ slightly larger than $10^{15}/\text{cm}^3$. They were lapped to an octagonal shape and the cross sectional areas were 0.13 cm². Typical results of applying axial stresses are shown in Fig. 2, where absorption derivatives are plotted *vs* magnetic field for the two different cases of zero stress and 3.5×10^7 dynes/cm² = 500 lb/inch². As the stress was increased the absorption derivative became shorter and broader. These results were reversible as would be expected since the strains are well within the elastic range.

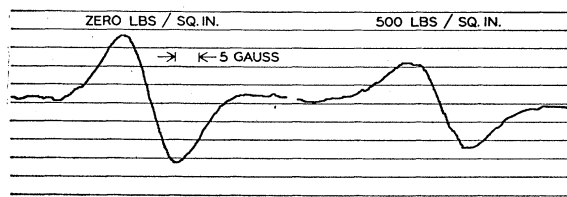


Fig. 2. Derivative of In¹¹⁵ absorption at different applied pressures.

Two sets of measurements were made on the crystal compressed along [110] and one set upon the [010] crystal. The second moment of the In¹¹⁵ absorption was measured for the [110] crystal with and without a stress of 3.5×10^7 dynes/cm². These measurements were made while the angle between [001] and H_0 , which we will designate as θ_x , was maintained at 0°. The results of these observations are presented in Table I. The ratios of the integrated intensities with and without stress are listed in the third column and the second moments of the upper and lower halves of the absorption line are shown in column four. The experimental results presented in this section will be interpreted in the following section.

In addition to the results of Table I, measurements were made on the [110] crystal as a function of the angle θ_x . Our apparatus records the derivative of the absorption. The peak-to-peak recorder deflection was measured as a function of θ_x and the normalized results are plotted in Fig. 3. All the points represent an average

TABLE I. Experimental values of second moments and relative intensities of In¹¹⁵ resonance for $H_0 = 8300$ oe for [110] compression, where $\theta_x = 0^\circ$.

Run No.	Stress dynes/cm ²	Relative Intensities 3.5×10^7 dynes/cm ²		ΔH^2 (gauss) ²	
		0 dynes/cm ²	Low field	High field	
IV	0	0.87	22.4	24.5	
II	3.5×10^7		30.3		29.7
V	0	0.89	24.4	24.7	
VI	3.5×10^7		32.8		38.4
VII	0	0.84	25.1	30.2	
VII	3.5×10^7		31.1		35.4
X	0	0.92	24.4	23.2	
XI	3.5×10^7		30.1		30.2
IX	3.5×10^7		31.5		32.5
Average		0.88	24.1	25.6	
			31.2	33.2	

of at least four measurements with applied stress and an equal number without. The unstressed line measured at each position was used to normalize the results. It had previously been determined³ that in the absence of compression the absorption was independent of crystal orientation and this, too, was confirmed in these measurements. In the following section we shall show how the quadrupole splitting may be related to the second moment which in turn may be expressed in terms of the recorder deflection if one assumes a line shape.

The [010] crystal presented a much simpler system and the only measurements made on this crystal were recorder deflection *vs* θ_x , where θ_x is still the angle between [001] and H_0 . This crystal did not show any dependence of recorder deflection upon angle as may be seen from Fig. 3.

INTERPRETATION

In order to understand the effects of applying elastic stress to the InSb it is necessary to describe what we

knew of the lines before stress was applied. In an early experiment³ the In¹¹⁵ resonance in a single crystal of InSb was examined before and after 20% plastic deformation. After deformation the integrated intensity had decreased by a factor of ~ 5 . If the effect of deformation was to remove all of the first-order quadrupole components leaving only the $m = -\frac{1}{2} \leftrightarrow +\frac{1}{2}$ transition, the intensity should have been reduced by a factor of 6.6. We took the decrease of intensity upon compression as an indication that the original intensity included contributions from transitions other than the $m = -\frac{1}{2} \leftrightarrow +\frac{1}{2}$. The numerical factor being close to the theoretical value of 6.6 meant that most of the first-order components were included in the original intensities.

Since we believed that all the components were present, we decided to remove them by destroying the cubic symmetry of the InSb zincblende structure in a reversible, controlled fashion. For example, a compressive stress along [010] will make the crystal tetragonal with the [010] as the unique axis. A stress applied along

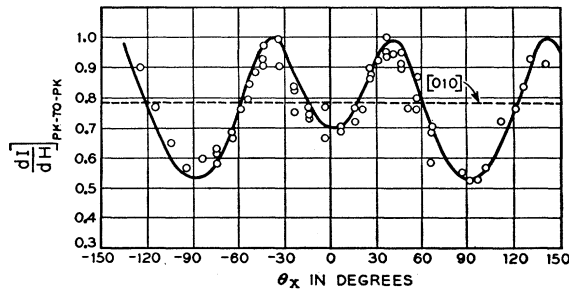


FIG. 3. Plot of $dI/dH]_{\text{peak-to-peak}}$ vs θ_x . Open circles are normalized experimental values of $dI/dH]_{\text{peak-to-peak}}$ for [110] compression while solid curve is best fit of $[1 + \sum_m A_m \delta_m^2]^{-1}$. The summation over m was taken as the average value of the sum from $m = -5/2$ to $7/2$ and the sum from $m = -7/2$ to $9/2$. The straight line is the average of 25 experimental values of $dI/dH]_{\text{peak-to-peak}}$ for [010] compression.

[110] makes the crystal orthorhombic, the three axes of twofold symmetry being the [110] along which we compress, the [001] perpendicular to this direction and the $[\bar{1}10]$ perpendicular to both. The strains can be calculated from recent determinations⁵ of the elastic constants of InSb, and are listed in Table II for compression along [110] and [010]. The electric-field gradient tensor ∇E will also lose its cubic symmetry, and, like the strain, becomes orthorhombic for [110] stress and tetragonal for [010].

Our object here is to relate the observed broadenings to the stress. This involves three steps: First, finding the splittings from our measurements; second, finding the field-gradient tensor in terms of the splittings; and third, relating this to the stresses. For the second step we use the following formula from Volkoff, Petch, and

TABLE II. Strain vs stress of 3.5×10^7 dynes/cm² along [010] and [110].

Stress \ Strain	3.5×10^7 dynes/cm ² along [110]	3.5×10^7 dynes/cm ² along [010]
E_{xx}	2.8×10^{-5}	-3.0×10^{-5}
E_{yy}	2.8×10^{-5}	$+8.5 \times 10^{-5}$
E_{zz}	-3.0×10^{-5}	-3.0×10^{-5}
E_{xy}	-5.9×10^{-5}	0
E_{xz}	0	0
E_{yz}	0	0

Smellie⁶:

$$(\Delta\nu)_m = \nu_{m \leftrightarrow (m-1)} - \nu_0 = \frac{3(2m-1)eQ}{4I(2I-1)\hbar} \varphi_{z'z'} = \frac{g\beta\delta_m}{\hbar}. \quad (1)$$

$\nu_{m \leftrightarrow (m-1)}$ is the frequency of an individual transition, and δ_m is its observed splitting in gauss; $\varphi_{z'z'}$ is the second derivative of the electrostatic potential at the nucleus along the z' axis parallel to the steady magnetic field H_0 ; and eQ is the nuclear quadrupole moment. The various components of the second derivative $\varphi_{z'z'}$, etc., form the field-gradient tensor, which must be made traceless, since its trace does not affect the frequency, and is symmetric, since $\nabla \times E = 0$. This tensor has five independent components in general; if we know its principal axes, though (as we do in our particular experiments), we need to know only two of the principal values. Relative to its principal axes, which we call x , y , and z , it may be written

$$\varphi = \begin{pmatrix} \varphi_{xx} & 0 & 0 \\ 0 & \varphi_{yy} & 0 \\ 0 & 0 & -(\varphi_{xx} + \varphi_{yy}) \end{pmatrix}.$$

In order to relate $\varphi_{z'z'}$ to φ_{xx} and φ_{yy} we need to transform x , y , z into x' , y' , and z' . In our experiments one of the principal axes of the tensor was, by symmetry, always the axis along which we applied compressive stress; let us call this $x = x'$. Then the field H_0 (i.e., z') was rotated in the plane yz perpendicular to x . Arbitrarily identifying one of the other two axes as z , the frequency as a function of the angle θ_x between the field z' and z is

$$\Delta\nu_{m \leftrightarrow m-1} = -\frac{3(2m-1)eQ}{8I(2I-1)\hbar} \times [\varphi_{zz} + (\varphi_{xx} + 2\varphi_{yy}) \cos 2\theta_x] \quad (2)$$

by simple transformation formulas.

For In¹¹⁵, Eq. (2) predicts a symmetrical pattern of nine components since $I = 9/2$. As mentioned above, the resonance lines were broadened in our experiments but the individual components were not separated. Therefore it was necessary to determine the quadrupole coupling parameter $eQ\varphi_{z'z'}$ for a given deformation and

⁵ R. F. Potter, Bull. Am. Phys. Soc. Ser. II, 1, 53 (1956); McSkimin, Bond, Pearson and Hrostowski, Bull. Am. Phys. Soc. Ser. II, 1, 111 (1956).

⁶ Volkoff, Petch, and Smellie, Can. J. Phys. 30, 270 (1952).

crystal orientation from the line shapes as follows. The second moments of the absorptions are defined as

$$\Delta H_2^2 = \int_{-\infty}^{\infty} x^2 I(x) dx, \quad (3)$$

where $x = H - H_0$ and $I(x)$ is the normalized intensity.

Since in the absence of strain the line breadth is determined primarily by exchange with the Sb nuclei,³ we can assume that the shapes of the individual components do not change with strain. Thus we can use the additive property of the second moment and obtain

$$\Delta H_2^2 = \Delta H_2^2(0) + \sum_m A_m \delta_m^2, \quad (4)$$

where $\Delta H_2^2(0)$ is the second moment of the unstrained crystal and A_m is the normalized relative intensity of the $m \leftrightarrow (m-1)$ transition.

By using Eq. (4) it is possible to convert changes of the second moment into values of δ_m and hence into $eQ\varphi_{z'z'}$. It was not possible to compute ΔH_2^2 for stresses much larger than 3.5×10^7 dynes/cm² because the tails of the distribution became too important and too uncertain. On the other hand very small stresses hardly changed the second moment and there too the errors were judged to be too large to enable $eQ\varphi_{z'z'}$ to be calculated. A series of runs with 3.5×10^7 dynes/cm² along [110] with $\theta_x = 0^\circ$ was the basis for calculating $eQ\varphi_{z'z'}$ at $\theta_x = 0^\circ$. The changes in ΔH_2^2 and integrated intensities observed under these conditions are listed in Table I. In the fourth column the second moments are listed for the low-field and high-field halves of the In¹¹⁵ line. It can be seen that the high-field half has a larger moment than the low half regardless of the stress. It is believed that In¹¹³, which is four percent abundant, and which for the frequencies used lies ~ 15 gauss higher, creates this slight asymmetry. The average increase of ΔH_2^2 is 7.4 gauss². In the third column we compare the relative intensities of the lines with and without deformation. It can be seen that 12% of the integrated intensity is lost during compression. The uncompressed comparisons were sometimes measured before the compression and sometimes after so that the intensity loss as well as the broadening are definitely reversible. From the matrix elements¹ one calculates that the $m = 7/2 \leftrightarrow 9/2$ and $-7/2 \leftrightarrow -9/2$ transitions contribute 11% to the total intensity. Therefore we assume for the initial calculation that these components have been spread too far and are lost in noise. Equation (4) was used in the form

$$\Delta H_2^2 = \Delta H_2^2(0) + \sum_{m=5/2}^{7/2} A_m \delta_m^2$$

to interpret these results. From the average increase of ΔH_2^2 at 3.5×10^7 dynes/cm² it was found that $eQ\varphi_{z'z'}$ at $\theta_x = 0^\circ = 44$ kc/sec. This value of quadrupole splitting indicates that the $|7/2| \leftrightarrow |9/2|$ transitions should be displaced six gauss which means that they

should contribute to the second moment which resulted from summing contributions as much as fifteen gauss away. A solution consistent with these displacements but inconsistent with the measured relative intensities would include the contributions of the $|7/2| \leftrightarrow |9/2|$ transitions. Including these terms the calculated value is 38 kc/sec. For the best estimate from these data $eQ\varphi_{z'z'}$ at $\theta_x = 0^\circ = 41$ kc/sec $\equiv eQ\varphi_{[001]}$.

In order to confirm the hypothesis of quadrupole splitting, the two samples were rotated about their compression axes and the peak-to-peak derivative intensities measured as a function of rotation. A variation of intensity with rotation was observed in the crystal compressed along [110] and rotated around this direction. For the purposes of rotation we identify the three principal axes of the field-gradient tensor in this crystal, [110], $[\bar{1}\bar{1}0]$, [001] with x , y , z respectively. In this way θ_x is the angle between [001] and H_0 .

Ideally one should plot ΔH_2^2 as a function of the angle θ_x , since Eq. (4) relates these quantities. Reasonable agreement between theory and experiment was found, however, by assuming the lines continue to be Gaussian under compression and this simpler approach is illustrated in Fig. 3. By assuming Gaussian lines $\delta H = 2[\Delta H_2^2]^{1/2}$, where δH is the full width between line derivative extremes. In addition, for Gaussians the product of the peak-to-peak recorder deflection and the square of the separation of the peaks is proportional to the integrated intensity. Combining this relation with Eq. (4) and assuming the integrated intensity to be constant, we have

$$\left. \frac{dI}{dH} \right|_{\text{peak-to-peak}} \propto [1 + \sum_m A_m \delta_m^2]^{-1},$$

where

$$\delta_m = \frac{h\Delta\nu_{m \leftrightarrow (m-1)}}{g\beta} \quad (5)$$

and $\Delta\nu_{m \leftrightarrow (m-1)}$ is defined by Eq. (2). Interpreting these results in the manner described above, we find the best fit to the data to be $eQ\varphi_{[110]} = \mp 16$ kc/sec; $eQ\varphi_{[001]} = \mp 36$ kc/sec and $eQ\varphi_{[110]} = \pm 52$ kc/sec. The solid curve in Fig. 3 has been calculated from these values.

As mentioned above, the [010] compression is simpler to interpret. For this case $\varphi_{yy} = \varphi_{zz} = -\frac{1}{2}\varphi_{xx}$. Therefore when the crystal is rotated about [010] there is no change in $\varphi_{z'z'}$. In this case, Eq. (2) reduces to Pound's formula¹:

$$\Delta\nu_{m \leftrightarrow m-1} = -\frac{3(2m-1)eQ}{8I(2I-1)}\varphi_{xx}(3\cos^2\theta - 1), \quad (6)$$

where θ is now the angle from (not around) the x axis. This explains the absence of orientation dependence shown as a straight line in Fig. 3 and enables one to calculate $eQ\varphi_{[010]} = \pm 60$ kc/sec and $eQ\varphi_{[100]} = eQ\varphi_{[001]}$

= ∓ 30 kc/sec. All the signs of the coupling parameters are undetermined by these measurements since the first-order quadrupole splitting is symmetric. However, the relations between the three coupling parameters for each compression are accurately described by the \pm and \mp signs. (Also, for the assignment of relative signs between the two see below.)

In the appendix we introduce the concept of "gradient-elastic" constants relating the field gradient to the applied stress by a linear tensor equation:

$$\varphi_{\mu\nu} - \varphi_{\mu\nu}^0 = \sum_{\kappa\lambda} C_{\mu\nu;\kappa\lambda} X_{\kappa\lambda}. \quad (7)$$

For the special case of a cubic site in a cubic crystal we show that the relationship (7) is particularly simple, involving only two constants C_{11} and C_{44} :

$$\begin{aligned} \varphi_{xx} &= C_{11} [X_{xx} - \frac{1}{2}(X_{yy} + X_{zz})], \\ \varphi_{xy} &= C_{44} X_{xy}, \end{aligned} \quad (8)$$

where x , y , and z are the usual cubic axes.

We shall not give explicitly the various transformations necessary to use (8) in the present case, but simply present the result: With a strain X along $[110]$, the field-gradient tensor is, in our previous notation, ($x=[110]$, $y=[\bar{1}\bar{1}0]$, $z=[001]$)

$$\varphi = \begin{pmatrix} (\frac{1}{4}C_{11} + \frac{1}{2}C_{44})X & 0 & 0 \\ 0 & (\frac{1}{4}C_{11} - \frac{1}{2}C_{44})X & 0 \\ 0 & 0 & -\frac{1}{2}C_{11}X \end{pmatrix}, \quad (9)$$

which, using the experimental values for this case, gives

$$\begin{aligned} eQC_{11} &= \mp 2 \times 10^{-6} (\text{kc/sec})(\text{cm}^2/\text{dyne}), \\ eQC_{44} &= \pm 2 \times 10^{-6} (\text{kc/sec})(\text{cm}^2/\text{dyne}), \end{aligned} \quad (10)$$

with an estimated accuracy of about $\pm 20\%$.

Using the known quadrupole moment of In^{115} , 1.161×10^{-24} cm², this can be converted to an actual field gradient:

$$\begin{aligned} C_{11} &= (\pm 2.4 \pm 0.5) \times 10^4 \text{ statvolts/dyne}, \\ C_{44} &= (\mp 2.4 \pm 0.5) \times 10^4 \text{ statvolts/dyne}. \end{aligned} \quad (11)$$

The compression along $[001]$ provides a check on these values using the theory of the gradient-elastic tensor, which may be expressed most simply as follows: in the cubic case (not generally—see appendix) the gradient-elastic tensor is symmetric. Therefore stress along $[110]$ should produce, along $[001]$, the same field-gradient tensor principal value that stress along $[001]$ gives along $[110]$. Thus the 30 kc/sec value obtained for $[010]$ stress must be compared with the 36 kc/sec obtained along $[001]$ with $[110]$ stress. The difference of 20% is of the order of our estimates of our experimental error.

It is interesting to compare the values (11) with crude estimates which we have made by assuming that a single electronic charge of appropriate sign is at each lattice point and that the deformation of the unit cell is uniform. Such an estimate involves a difficult lattice

sum of which we did only the first three shells. The first shell gives $C_{11} = 380$ esu/dyne; the second, -100 ; and the third, $+40$. Clearly the sum does not converge rapidly, but a figure like 350 esu/dyne represents a likely order of magnitude. Thus we have an anti-screening factor of at least 70. The true factor is even larger since we have assumed an effective charge much larger than that which is present, and ignored screening. However, the true cause of the effect is more likely to be a change in the bonding orbitals than motion of the charges on the "ions."

Finally we should like to report that qualitatively the same results have been obtained with a single crystal of GaSb.

CONCLUSIONS

1. The cubic symmetry of single-crystal InSb has been destroyed by elastic deformation and line broadening from quadrupole interactions observed.

2. Strains of less than 10^{-4} are readily detectable by this kind of measurement. This compares well with the best mechanical strain gauges.

3. The nuclear magnetic resonance method of detecting strain is localized so that one may observe electric field gradients at different lattice sites by observing different nuclear transitions.

4. It has been possible to detect the quadrupole effects that are caused by elastic deformation alone. Therefore it should be possible to use this type of measurement to determine crystalline perfection.

5. It has been shown that the change in electric-field gradient at the nucleus upon compression is ~ 70 times too large to be explained by the displacement of charge considering all constituents to be ionic.

6. The relations between stress and field gradients have been derived and are shown to be consistent with the observations.

ACKNOWLEDGMENT

It is a pleasure to thank Dr. H. J. Hrostowski for the excellent single crystals of InSb which made these experiments possible.

APPENDIX

There is a close analogy between the problem of the effect of stress on the field-gradient tensor as measured by quadrupole splitting and the theory of crystalline elastic constants.

The elastic-constant tensor is a linear relationship c connecting the stress tensor $X_{\mu\nu}$ with the strain $x_{\kappa\lambda}$:

$$x_{\kappa\lambda} = \sum_{\mu,\nu} c_{\kappa\lambda;\mu\nu} X_{\mu\nu}; \quad (A1)$$

κ , λ , μ , and ν all run over x , y , and z . Since x and X are necessarily symmetric tensors they each have only 6 independent components, giving only 36 rather than 81 meaningful components of c . For convenience, (A1) is

often written in the misleading notation⁷:

$$x_j = \sum_k c_{jk} X_k, \quad j, k = 1 \cdots 6, \quad (\text{A2})$$

$$\begin{aligned} 1 &= xx, & 4 &= yz, \\ 2 &= yy, & 5 &= zx, \\ 3 &= zz, & 6 &= xy, \end{aligned} \quad (\text{A3})$$

which is briefer but de-emphasizes the important fact that x , X , and c are 2-, 2-, and 4-index tensors, respectively. Conservation of energy further simplifies (A1) or (A2) by requiring that c be symmetric in j and k , which leaves it with at most 21 independent components.

For crystals of any greater symmetry than the very lowest (A1) or (A2) can be simplified by taking this further symmetry into account: that is, one requires that the quantities x , X , and c transform in the proper way under rotations, while at the same time (A1) must not change under symmetry rotations of the crystal. For example, any cubic point-group symmetry can be shown to require

$$\begin{aligned} c_{11} &= c_{22} = c_{33}, \\ c_{44} &= c_{55} = c_{66}, \quad \text{all others} = 0, \\ c_{12} &= c_{23} = c_{31}, \end{aligned} \quad (\text{A4})$$

while for trigonal or hexagonal symmetry

$$\begin{aligned} c_{11} &= c_{22}, \quad c_{13} = c_{23}, \quad c_{44} = c_{55}, \quad c_{66} = \frac{1}{2}(c_{11} - c_{12}); \\ &\text{all others but } c_{33} \text{ and } c_{12} = 0. \end{aligned} \quad (\text{A5})$$

Since elastic strains are so small it is certain that in the present experiments the change in the field-gradient tensor is a linear function of elastic stress or strain:

$$\varphi_{\mu\nu} - \varphi_{\mu\nu}^0 = \sum_{\kappa, \lambda} C_{\mu\nu; \kappa\lambda} X_{\kappa\lambda}, \quad (\text{A6})$$

where $\varphi_{\mu\nu}^0$ is the field-gradient tensor at the site of interest in the absence of the stress X . Since X and φ are symmetric tensors, C has at most 36 independent components and thus it can be written in the Voigt notation:

$$\Delta \varphi_j = \sum_{k=1}^6 C_{jk} X_k. \quad (\text{A7})$$

Since the trace of the field-gradient tensor is unobservable we may as well set it equal to zero and as a result we have another requirement on C :

$$\sum_{\mu} \varphi_{\mu\mu} = \sum_{\mu} \sum_{\kappa, \lambda} C_{\mu\mu; \kappa\lambda} X_{\kappa\lambda} = 0,$$

which, since X is arbitrary, implies

$$\sum_{\mu} C_{\mu\mu; \kappa\lambda} = 0, \quad (\text{A8})$$

⁷ W. Voigt, *Lehrbuch der Kristallphysik* (Teubner, Leipzig, 1910).

or in Voigt's notation

$$\sum_{j=1}^3 C_{jk} = 0, \quad (\text{A8}')$$

leaving C with 30 independent components. Unfortunately, there is no such energy-conservation principle here as in the elastic case and so C need *not* be symmetric in j and k .

In a symmetric crystal (A6) must not change under symmetry operations of the point group of the site under consideration (although this group may of course be much less symmetric than the total point group of the crystal). This will often lead to simplifications.

So far the discussion is quite general. The case at hand, however, is the specific one of a site of tetrahedral (= cubic for even-order tensors) symmetry in a cubic crystal, in which all of the quadrupole splitting is caused by stress. Because of the asymmetry of C we cannot immediately use (A4) but must start over again. However, re-examination of the arguments on which (A4) is based⁸ reveals that C need not be totally symmetric in order to prove that

$$\begin{aligned} C_{11} &= C_{22} = C_{33}, \\ C_{44} &= C_{55} = C_{66}, \\ C_{12} &= C_{23} = C_{31} = C_{13} = C_{32} = C_{21}; \\ &\text{all others} = 0. \end{aligned} \quad (\text{A9})$$

To these conditions we may add (A8)

$$\begin{aligned} C_{11} + C_{12} + C_{13} &= 0, \\ C_{11} &= -2C_{12}, \end{aligned} \quad (\text{A10})$$

and there turn out to be only two independent gradient-elastic constants. The final result is the relationship, for our cubic case, of field gradient to stress,

$$\begin{aligned} \varphi_{xx} &= C_{11}(X_{xx} - \frac{1}{2}X_{yy} + X_{zz}) \text{ (cyclic),} \\ \varphi_{xy} &= C_{44}X_{xy} \text{ (cyclic),} \end{aligned} \quad (\text{A11})$$

which is used in the text. The x , y , and z axes are taken to be the cubic axes.

Measurements such as those in the text determine the constants C_{11} and C_{44} (or the larger number of C 's for less symmetrical situations). Such measurements on perfect crystals would then allow one to interpret results on less perfect crystals in terms of internal strains⁹ if the effects of charged imperfections could be discounted.

⁸ F. Fumi, *Acta Cryst.* **1**, 44 (1952). We are indebted to J. C. Phillips for this reference and the above observation.

⁹ F. Reif, *Phys. Rev.* **100**, 1597 (1955).